

AEDC-TR-68-135

ARCHIVE COPY
DO NOT LOAN

By

WALL COOLING EFFECTS ON AXISYMMETRIC
LAMINAR REATTACHING FLOWS
AT HYPERSONIC SPEEDS



J. Don Gray
ARO, Inc.

November 1968

This document has been approved for public release
and sale; its distribution is unlimited.

VON KÁRMÁN GAS DYNAMICS FACILITY
ARNOLD ENGINEERING DEVELOPMENT CENTER
AIR FORCE SYSTEMS COMMAND
ARNOLD AIR FORCE STATION, TENNESSEE

AEDC TECHNICAL LIBRARY



5 0720 00062 7614

PROPERTY OF U. S. AIR FORCE
AEDC LIBRARY
F40690 - 69 - C - 0001

NOTICES

When U. S. Government drawings specifications, or other data are used for any purpose other than a definitely related Government procurement operation, the Government thereby incurs no responsibility nor any obligation whatsoever, and the fact that the Government may have formulated, furnished, or in any way supplied the said drawings, specifications, or other data, is not to be regarded by implication or otherwise, or in any manner licensing the holder or any other person or corporation, or conveying any rights or permission to manufacture, use, or sell any patented invention that may in any way be related thereto.

Qualified users may obtain copies of this report from the Defense Documentation Center.

References to named commercial products in this report are not to be considered in any sense as an endorsement of the product by the United States Air Force or the Government.

WALL COOLING EFFECTS ON AXISYMMETRIC
LAMINAR REATTACHING FLOWS
AT HYPERSONIC SPEEDS

J. Don Gray

ARO, Inc.

This document has been approved for public release
and sale; its distribution is unlimited.

FOREWORD

This work was done at the request of the Air Force Flight Dynamics Laboratory (AFFDL), Flight Controls Division, Air Force Systems Command (AFSC), for the Nielsen Engineering and Research Company (NEAR) under Program Element 6240533F, Project 8219, Task Number 821902.

The results of tests presented were obtained by ARO, Inc. (a subsidiary of Sverdrup & Parcel and Associates, Inc.), contract operator of the Arnold Engineering Development Center (AEDC), Air Force Systems Command (AFSC), Arnold Air Force Station, Tennessee, under Contract F40650-69-C-0001. The work was accomplished under ARO Project Number VT0756, and the manuscript was submitted for publication on May 29, 1968. The contributions of W. R. Prater in the development of the special pressure measuring system used during this test are gratefully acknowledged. The tests were conducted intermittently in periods between December 1967 and April 22, 1968.

This technical report has been reviewed and is approved.

Donald H. Meyer
Major, USAF
AF Representative, VKF
Directorate of Test

Roy R. Croy, Jr.
Colonel, USAF
Director of Test

ABSTRACT

A flared (10-deg semiangle) axisymmetric body was tested at Mach 6, 8, and 10 in the von Kármán Gas Dynamics Facility to investigate the effect of model wall temperature on the existence of laminar flow separation and reattachment. The results consisted of longitudinal surface pressure distributions obtained at zero incidence. By varying the stagnation pressure, the influence of the free-stream Reynolds number on the extent of flow separation was also investigated. Extensive measurements were made at Mach 8 for Reynolds numbers (based on centerbody diameter) ranging from about 0.05 to 0.29 million and at wall temperatures from about 0.1 to 0.8 times the free-stream stagnation temperature. The results show that wall cooling increased substantially the pressure gradients at the separation and reattachment locations. The size of the interaction region (upstream influence) was found to decrease systematically with decreasing wall temperature ratio (Reynolds number constant) and to increase with increasing Reynolds number (constant wall temperature ratio). The effect of free-stream Mach number on the upstream influence (at fixed local Reynolds number and wall temperature) was indicated to be negligible.

CONTENTS

| | <u>Page</u> |
|---------------------------------------|-------------|
| ABSTRACT | iii |
| NOMENCLATURE | vii |
| I. INTRODUCTION | 1 |
| II. APPARATUS | |
| 2.1 Wind Tunnels | 2 |
| 2.2 Models | 2 |
| 2.3 Instrumentation | 4 |
| 2.4 Testing Procedures | 6 |
| III. RESULTS AND DISCUSSION | 7 |
| REFERENCES | 24 |

ILLUSTRATIONS

Figure

| | |
|--|----|
| 1. Model Geometry | 3 |
| 2. Model Installation in Tunnel B | 4 |
| 3. Transducer Package Components | 5 |
| 4. Surface Pressure Distributions at Different Reynolds Numbers for Near Ambient Wall Temperature | |
| a. Mach 8 | 8 |
| b. Mach 6 | 9 |
| 5. Surface Pressure Distributions for Interaction Region Upstream of Flare at Mach 8 for Near Ambient Wall Temperature at Zero Incidence | |
| a. Referenced to Free-Stream Pressure | 10 |
| b. Referenced to Pressure at Beginning of Interaction | 10 |
| 6. Surface Pressure Distributions for Mach 8 with Near Adiabatic Wall Temperature | 12 |
| 7. Effect of Roll Angle on Surface Pressure Distribution for Near Ambient Wall Temperature at Mach 10 | 13 |
| 8. Surface Pressure Distributions at Different Mach Numbers for Near Ambient Wall Temperatures | |
| a. Low Reynolds Number, $0.069 \leq Red \times 10^{-6}$ ≤ 0.083 | 14 |
| b. High Reynolds Number, $Red \approx 0.25 \times 10^6$ | 15 |

| <u>Figure</u> | <u>Page</u> |
|---|-------------|
| 9. Surface Pressure Distributions at the Wall Temperature Extremes | |
| a. Mach 8, Maximum Reynolds Number | 17 |
| b. Mach 8, Minimum Reynolds Number | 18 |
| c. Mach 6, Maximum Reynolds Number | 19 |
| d. Mach 6, Minimum Reynolds Number | 20 |
| 10. Variation of the Upstream Influence with Reynolds Number and Heat Transfer at Mach 8 and Zero Incidence | |
| a. Wall Temperature Ratio Constant | 21 |
| b. Reynolds Number Constant | 21 |
| 11. Shadowgraph Pictures at Mach 8 for Different Wall Temperatures at $Re_d = 0.23 \times 10^6$ | |
| a. Near Ambient Wall Temperature $(T_w/T_o - 0.4)$ | 22 |
| b. Minimum Wall Temperature $(T_w/T_o - 0.1)$ | 22 |
| 12. Shadowgraph Pictures at Mach 6 for Different Wall Temperatures at $Re_d = 0.17 \times 10^6$ | |
| a. Near Ambient Wall Temperature $(T_w/T_o - 0.7)$ | 23 |
| b. Minimum Wall Temperature $(T_w/T_o - 0.3)$ | 23 |

NOMENCLATURE

| | |
|------------|---|
| C_p | Surface pressure coefficient, $(p - p_\infty)/q_\infty$ |
| d | Model centerbody diameter, 1.00, in. |
| M | Mach number |
| p | Static or surface pressure, psia |
| q_∞ | Free-stream dynamic pressure, psia |
| Re_d | Free-stream Reynolds number based on centerbody diameter |
| r | Local radius, in. |
| S | Surface distance relative to flare leading edge, positive downstream, in. |
| T_o | Tunnel stilling chamber temperature, °R |
| T_w | Surface temperature, °R |
| x | Axial distance, in. |
| α | Angle of attack, deg |
| ϕ | Roll angle, deg |

SUBSCRIPTS

| | |
|----------|---|
| 0 | Beginning of interaction between boundary layer and external flow |
| ∞ | Free stream |

SECTION I INTRODUCTION

An experimental examination of the effect of surface cooling on flare-induced, laminar flow separation was conducted at hypersonic speeds. These tests were made for the Nielsen Engineering and Research Company in order to provide data for comparison with theoretical results being developed under a contract with the Air Force Flight Dynamics Laboratory.

The original work of Nielsen, et al. (Ref. 1) showed that if the model wall temperature were below some critical percentage of the free-stream total temperature, separation would cease to exist for a free interaction between the boundary layer and the external flow. Their calculations for the case of "first-order coupling" indicated that a wall temperature which was less than a fourth of the stagnation temperature would suffice at Mach numbers of six or above and that this critical ratio was independent of Reynolds number. The "second-order coupling" theory, also derived in Ref. 1, is the theory with which the results of this test will be compared. This second theory differs from the first primarily in that it allows total temperature gradients to exist between the zero velocity line and the wall in the region between separation and reattachment.

The configuration used in this investigation was chosen on the basis of the results in Ref. 2. The nose configuration, however, was modified to reduce the flow expansion at the junction, and the centerbody was lengthened. Both of the changes were made to produce a more uniform flow field in the region approaching the flare.

Because preliminary investigations with an internally cooled model indicated that even moderately uniform longitudinal temperature distributions were extremely difficult to realize in a continuous flow hypersonic wind tunnel, a technique which would use a heat-sink type model and the model injection system was investigated and developed. For short exposures, it was found possible to achieve quite uniform model temperatures; and by using fast response transducers, the pressures could be measured during the short time available.

Feasibility tests for the pressure system were conducted in April 1967, and shakedown tests of the specially built pressure package were conducted at Mach 6 in November 1967. Tests were then conducted at Mach 6, 8, and 10 during the period from December 1967 through April 22, 1968, with the primary emphasis placed on obtaining comprehensive data at Mach 8.

SECTION II APPARATUS

2.1 WIND TUNNELS

Tunnels B and C are continuous, closed-circuit, variable density wind tunnels having 50-in. -diam contoured axisymmetric nozzles and model injection systems.

Tunnel B has a Mach 6 throat and a Mach 8 throat (for which the nozzle was designed). It can be operated at stagnation pressures from about 20 to 300 psia at Mach 6 and from 50 to 900 psia at Mach 8. The stagnation temperatures vary from about 390°F at Mach 6 to a maximum of about 900°F at Mach 8.

Tunnel C has a Mach 10 throat with a nozzle designed for that Mach number, and it can be operated at stagnation pressures from 200 to 2000 psia and stagnation temperatures up to about 1450°F.

A more complete description of the tunnels may be found in Ref. 3.

2.2 MODELS

The model geometry and the important details of the model used with the fast-response pressure system are shown in Fig. 1. The model had 41 pressure orifices located as shown in the bottom view. A removable 1/8-in. cover plate, sealed with an O-ring, was provided on the side opposite the orifices to allow access to the three thermocouples and to permit installation of the tubing. The aft centerbody section and the flare were machined from one piece of beryllium copper. The body extension and ogival nose were made from the same material, but the nose was plated to minimize erosion of the surface. The model was supported by a sting which was connected to the transducer package, as shown by the photograph of the model on the tunnel centerline in Fig. 2.

A second model was tested to obtain some data at near adiabatic wall temperatures. This model was the same one used in Ref. 2. Since the centerbody diameters were the same, the ogival nose was interchanged between the two models.

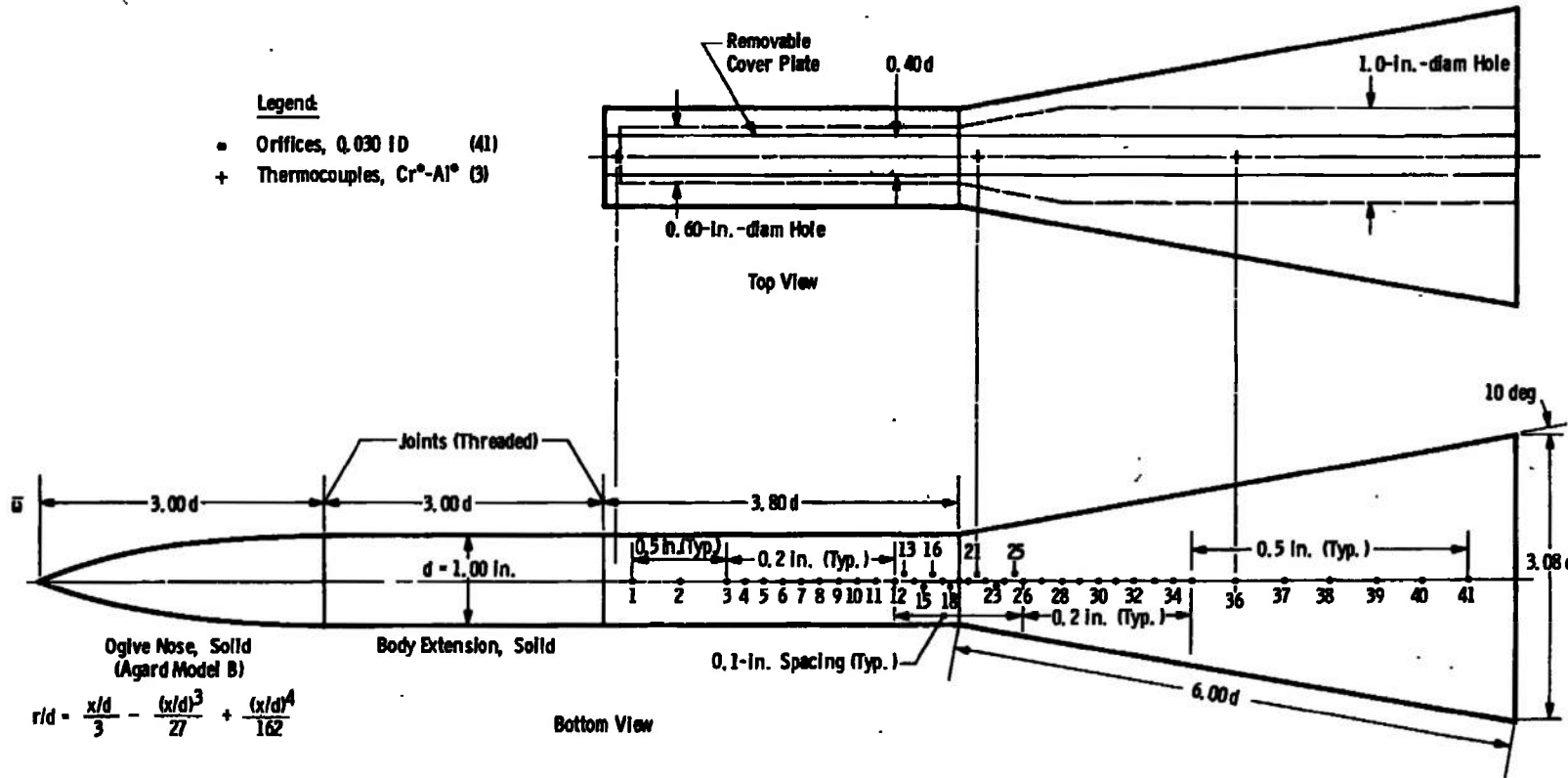


Fig. 1 Model Geometry

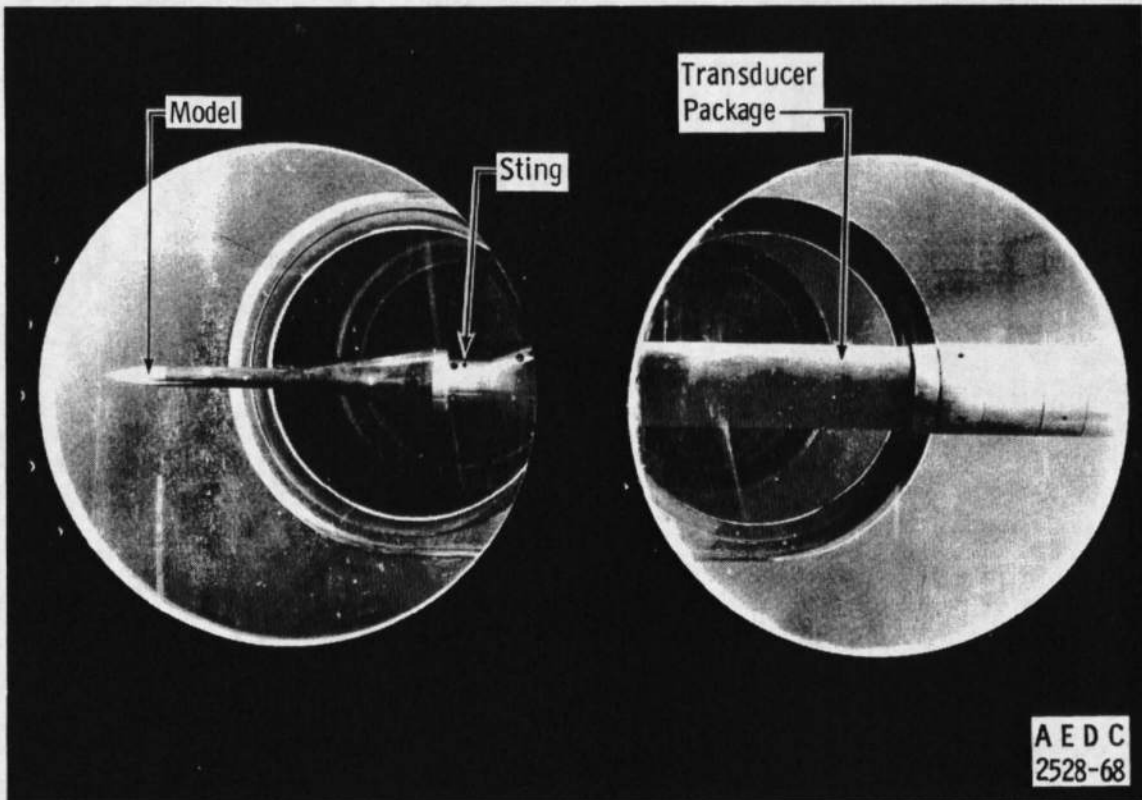


Fig. 2 Model Installation in Tunnel B

2.3 INSTRUMENTATION

The primary pressure measurements were obtained using a fast-response pressure system developed specifically to satisfy the requirement for surface pressure data at isothermal model wall conditions. A transducer package, components of which are shown in Fig. 3, was designed to provide a controlled environment for the transducers and also to serve as a model support. The package (4-in. OD) was sealed such that the internal pressure could be varied, and water was circulated through the passage between the inner and outer shells to provide a stable interior temperature (approximately 70°F). A connector plate at the upstream end of the package joined the model tubing to the transducer tubing. The combined length of tubing was no more than about two feet for any orifice. A variable-reluctance wafer gage of ± 0.5 -psid capacity was used for each orifice, and carrier amplifiers having variable attenuation conditioned the transducer signal before recording in digital form on magnetic tape.

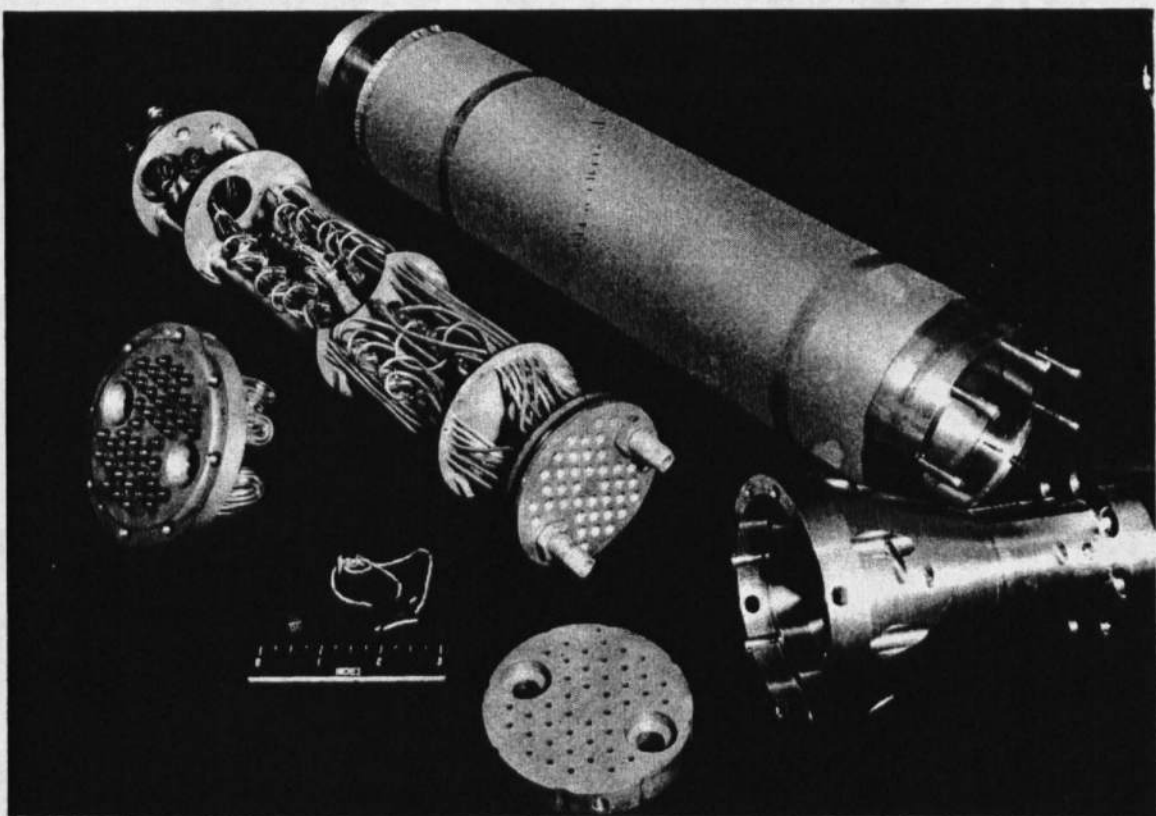


Fig. 3 Transducer Package Components

The leads from three Chromel®-Alumel® thermocouples, which were embedded in the model mass just under the cover plate (as located in Fig. 1), were carried through two 0.25-in. tubes which passed through the pressure package. The leads from two Gardon heat gages installed on the flare were also run through these tubes. These heat gages were installed with the expectation of deducing the onset of transition from changes in heat-transfer rate. During initial tests, one developed an electrical short, and the other produced inconclusive results. Because adequate indications of the state of the boundary layer during flow re-attachment were provided by the shadowgraph system, no heat-gage data will be presented.

The pressure measurements obtained at near adiabatic wall temperature conditions were made with the standard Tunnel B FM-type pressure transducer system using the model from Ref. 2.

Based upon a comparison of numerous repeated test conditions using the fast-response pressure system, the repeatability of individual measurements was less than ± 0.002 psi when the zero shift measured over the injection cycle was less than 0.0001 psi. Similar spreads in

repeatability were observed with the standard transducer system. Moreover, no definable deviation of these repeatability bands with tunnel pressure level variation was observed. In terms of pressure coefficient, this repeatability corresponds to a band of approximately ± 0.001 .

Temperature repeatability was considerably less than one degree. However, there is some question about the absolute error at temperatures in the neighborhood of liquid nitrogen temperature (-320°F) because measurements as much as 5°F lower were sometimes recorded. This situation often occurred even though the model temperature was steady with time during the cooling phase; the steady temperature was interpreted as proof of having reached the temperature of liquid nitrogen.

2.4 TESTING PROCEDURES

When using the fast-response pressure system, calibrations of all transducers were made frequently. A calibration pressure was applied by raising the pressure inside the transducer package to a value no more than 0.5 psi above the ambient pressure existing in the model-injection tank. This calibration pressure differential was simultaneously measured with a high resolution standard transducer. A zero pressure differential was also recorded by venting the transducer package through suitable valving to obtain ambient tank conditions on both sides of all transducers.

During testing, the standard transducer was used to establish the absolute reference pressure level for the wafer transducers. Just before model injection, the transducer package was vented briefly to the near free-stream pressure prevailing in the tank to seal in a stable reference pressure. Then, with the standard transducer referenced to a hard vacuum, the ambient tank pressure was recorded.

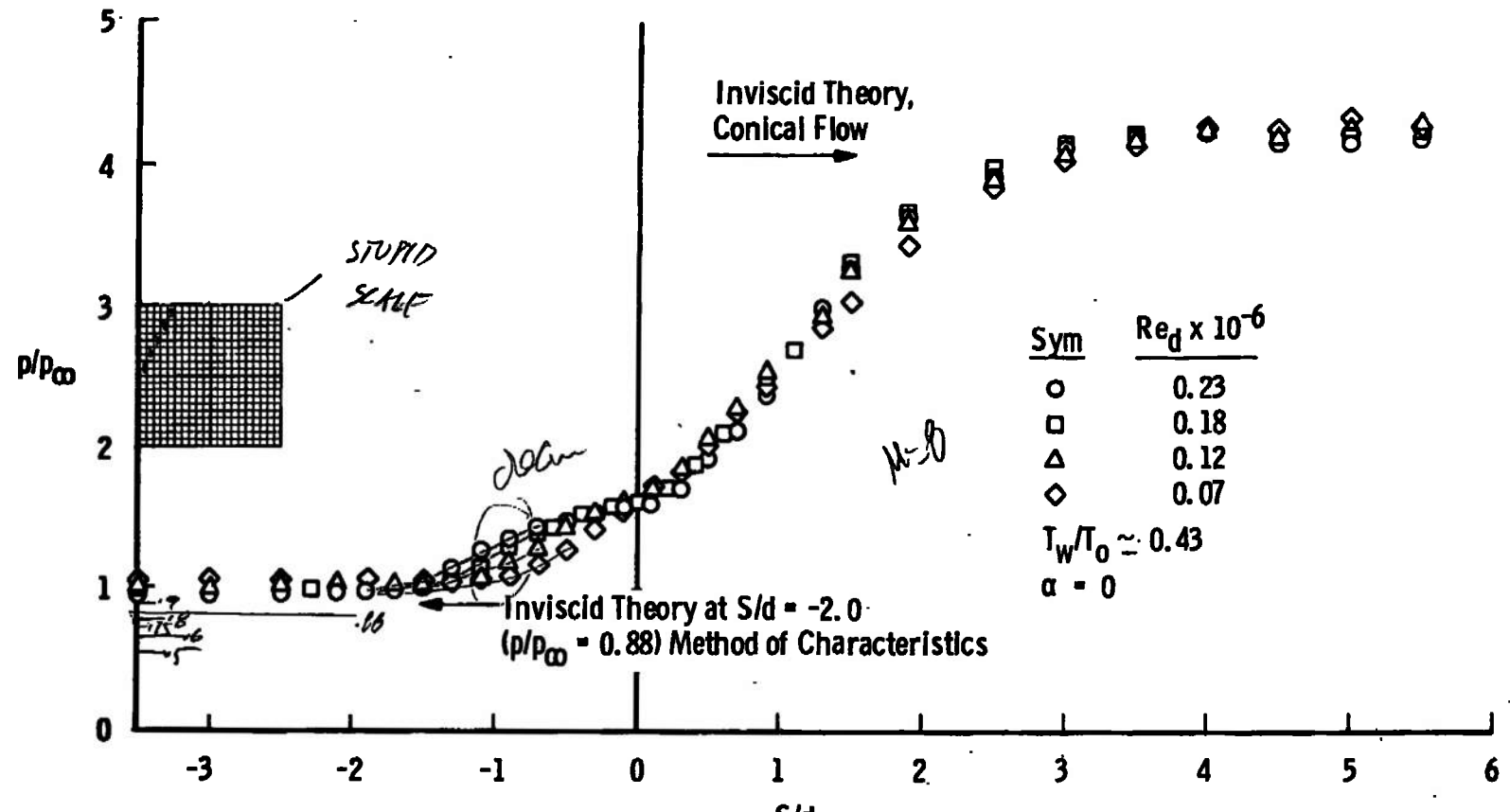
When the model was retracted, the wall temperature was varied from about 100°F to about -320°F by spraying the model with liquid nitrogen through a perforated manifold which ran along both sides and by spraying dry, high-pressure air toward the nose of the model through a nozzle in the tank door. This nozzle was closely aligned with the axis of the model and was used to control the level of temperature as well as to blow off frost accumulations. Whenever frost was allowed to take on the appearance of a sheet of thin ice (rather than a slightly glazed condition), it would clearly affect the pressure measurement if it formed over the orifices. However, with experience, it became relatively easy to obtain the minimum temperature without significant frost formation. Longitudinal temperatures uniform to within $\pm 5^{\circ}\text{F}$ were easily obtained at all temperature levels investigated.

The model incidence was set at zero (± 3 min) with respect to the tunnel centerline and was frequently checked, not only with an inclinometer set on the centerbody but also with a precision transit when the model was injected into the airstream. The zero roll reference position was defined to be with the orifices on the bottom side since it was expected that the liquid nitrogen spray might overload the transducers. The cooling procedure, however, caused no such problem when the model was rolled to $\phi = 180$ deg.

SECTION III RESULTS AND DISCUSSION

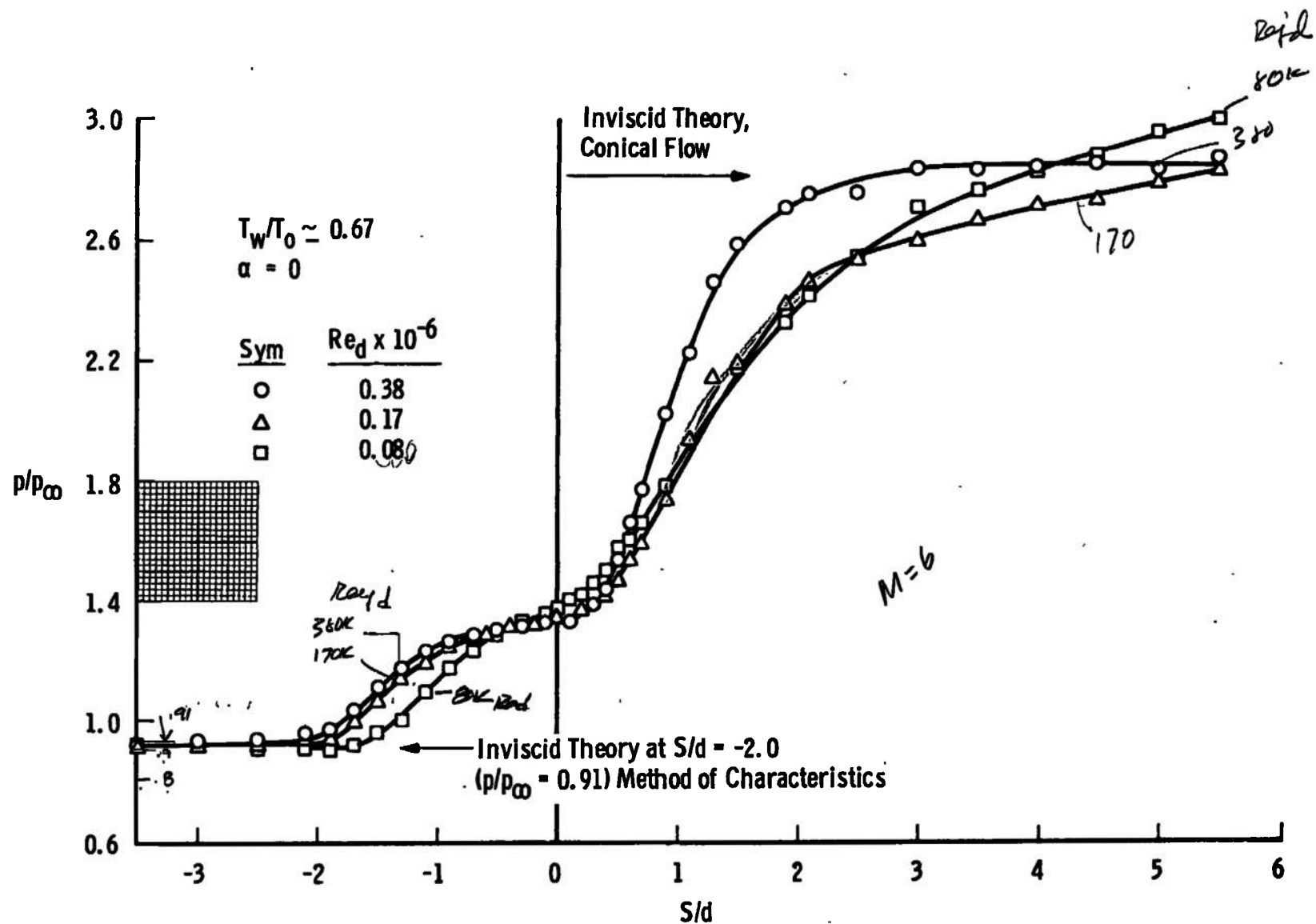
The effects of Reynolds number at essentially ambient (approximately 80°F) wall temperature are illustrated by the results in Fig. 4. It may be observed that the longitudinal station at which the pressure began to rise was moved upstream by a Reynolds number increase. This trend is characteristic of laminar flow separations which remain laminar through reattachment (see Ref. 2). Another characteristic of laminar reattaching flows, adequately demonstrated for the first time for wedge-type separations in Ref. 4, is shown by the data in Fig. 4a. That is, the pressure gradient on the flare is approximately constant when the flow is laminar through reattachment. However, when transition first approaches, the gradient becomes highly sensitive to Reynolds number. Thus, the distribution shown in Fig. 4b for Mach 6 at $Re_d = 0.38 \times 10^6$ should be classed as a transitional reattachment (this is also verified by shadowgraph pictures to be presented later). The theoretical estimates included in these figures verify the observed conditions upstream and downstream of the interaction region.

The consistency of the results and the high resolution of the pressure measurements are illustrated by the Mach 8 data in the region of flow separation from Fig. 4a plotted to an enlarged scale in Fig. 5. Since there was some effect of Reynolds number on the centerbody pressure ratio upstream of the primary interaction (as shown in Fig. 5a), these data were nondimensionalized by the pressure at the beginning of the interaction (Fig. 5b) to illustrate more clearly the slight variation of the peak pressure ratio with Reynolds number (in this case at the corner: $S/d = 0$). Furthermore, these data (Fig. 5b) show that the maximum pressure gradient was also only slightly affected by the three-fold Reynolds number change. The absence of any inflection in the pressure rise prior to the corner at $Re_d = 0.07 \times 10^6$ clearly shows that significant separation, that is, the reverse flow region, had ceased to exist at that condition.

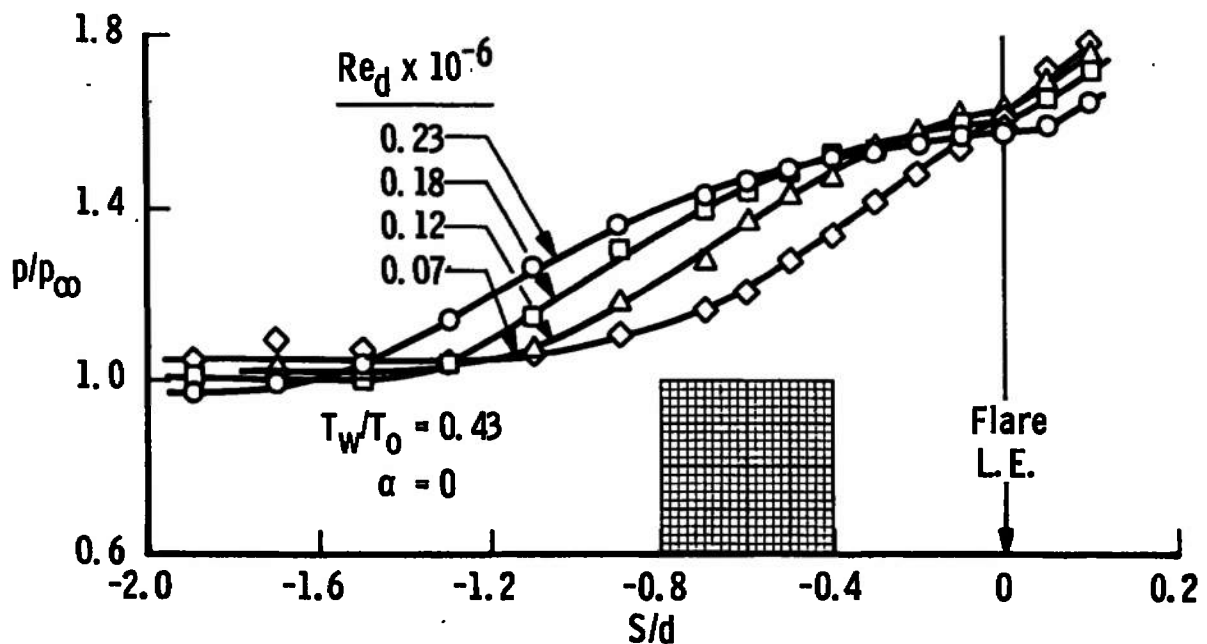


a. Mach 8

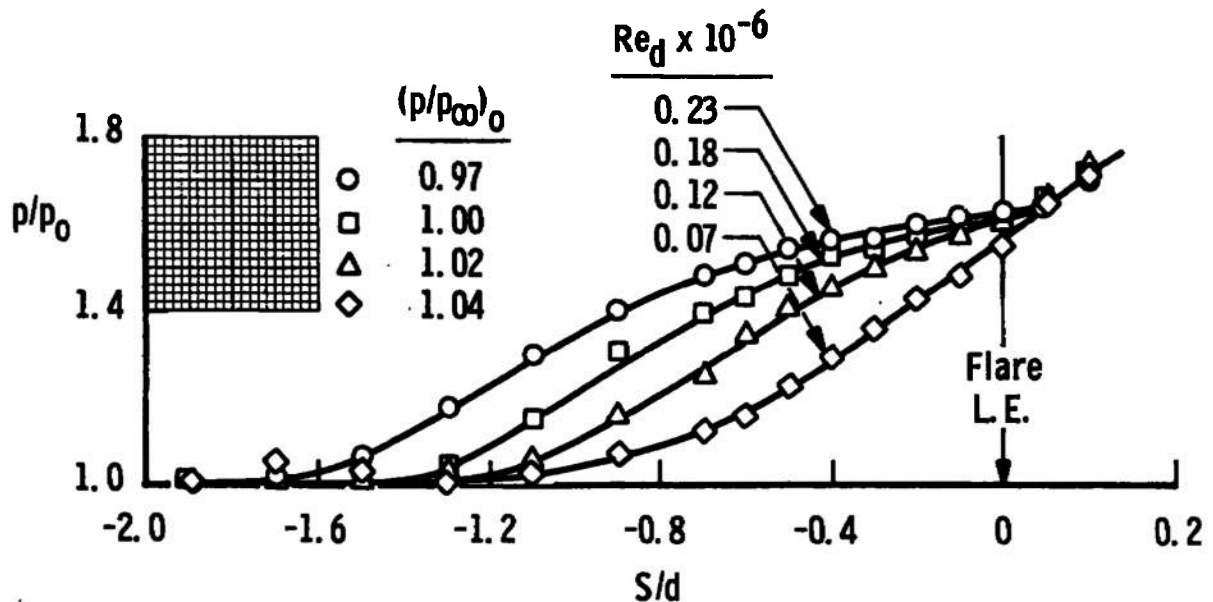
Fig. 4 Surface Pressure Distributions at Different Reynolds Numbers
for Near Ambient Wall Temperature



b. Mach 6
 Fig. 4 Concluded



a. Referenced to Free-stream Pressure



b. Referenced to Pressure at Beginning of Interaction

Fig. 5 Surface Pressure Distributions for Interaction Region Upstream of Flare at Mach 8 for Near Ambient Wall Temperature at Zero Incidence

The pressure distributions obtained at Mach 8 using the standard pressure measuring system are given in Fig. 6 in terms of the pressure coefficient. In this case, the model was allowed to approach an equilibrium temperature before taking data. These data show the laminar trend of an increased upstream interaction for an increase in Reynolds number, but a comparison of these results with those in Fig. 4a shows that the interaction region was considerably increased when the wall temperature was increased.

The most significant effect of rolling the model (at $\alpha = 0$) was found at Mach 10. These data are presented in Fig. 7, and the estimated mean values of C_p are given by the curve. The change attributable to roll at Mach 6 and 8 was on the order of the repeatability and, thus, insignificant. Since the effect of a 0.5-deg incidence change was found to move separation downstream and reattachment upstream on the windward side (conversely on the leeward side), the results shown here can hardly be attributed to flow angularity. Nevertheless, the tests at Mach 10 were terminated early because these results (at the maximum available Reynolds number) indicated that the incipient separation condition was being closely approached.

The effects of Mach number on the flare-induced interaction are illustrated by the data in Fig. 8 for an approximately constant free-stream Reynolds number. A most interesting, and perhaps quite surprising, point to note is the independence of the reattachment pressure distribution at fixed Reynolds number. The maximum pressure gradient upstream of the flare, although nominally the same, does, nevertheless, show the correct trend with Mach number. It was shown in Ref. 2 that this gradient in two-dimensional flow is increased by increasing either the wall cooling or the Mach number, although the latter effect was indicated to be negligible at $M \geq 8$. There does appear to be, however, a rather substantial decrease in the upstream influence for the Mach number increase shown. It may also be seen that there was a fairly large effect of Mach number on the centerbody pressure upstream of the separation region, and this may account, in part, for the observed effects. As will be seen in the next figures, the wall temperature has an important influence on the scale of the interaction. Since the stagnation temperature was increased as the Mach number was increased, the wall temperature ratio decreased such that the decrease in the separation extent shown in Fig. 8 cannot be ascribed solely to Mach number.

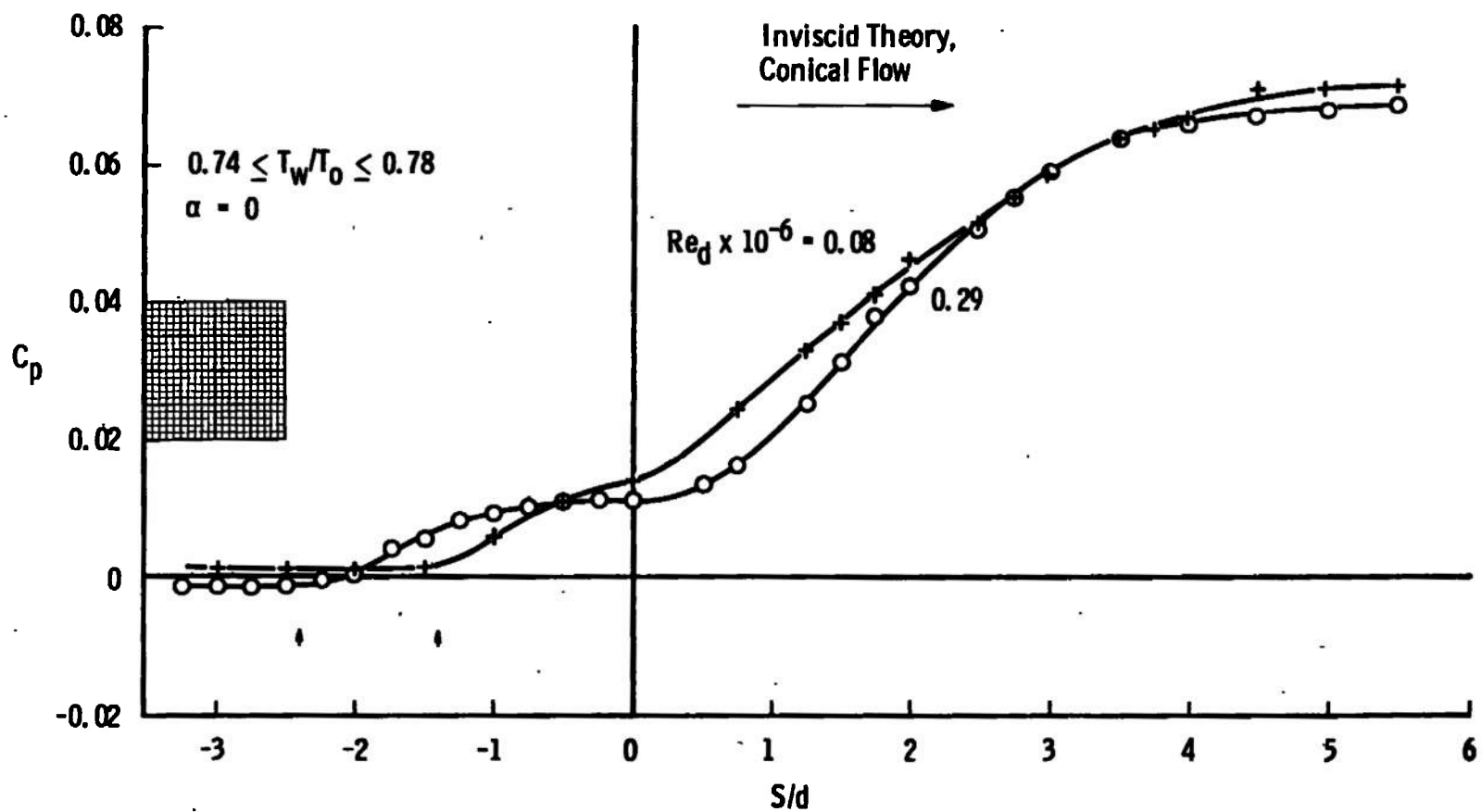


Fig. 6 Surface Pressure Distributions for Mach 8 with Near Adiabatic Wall Temperature

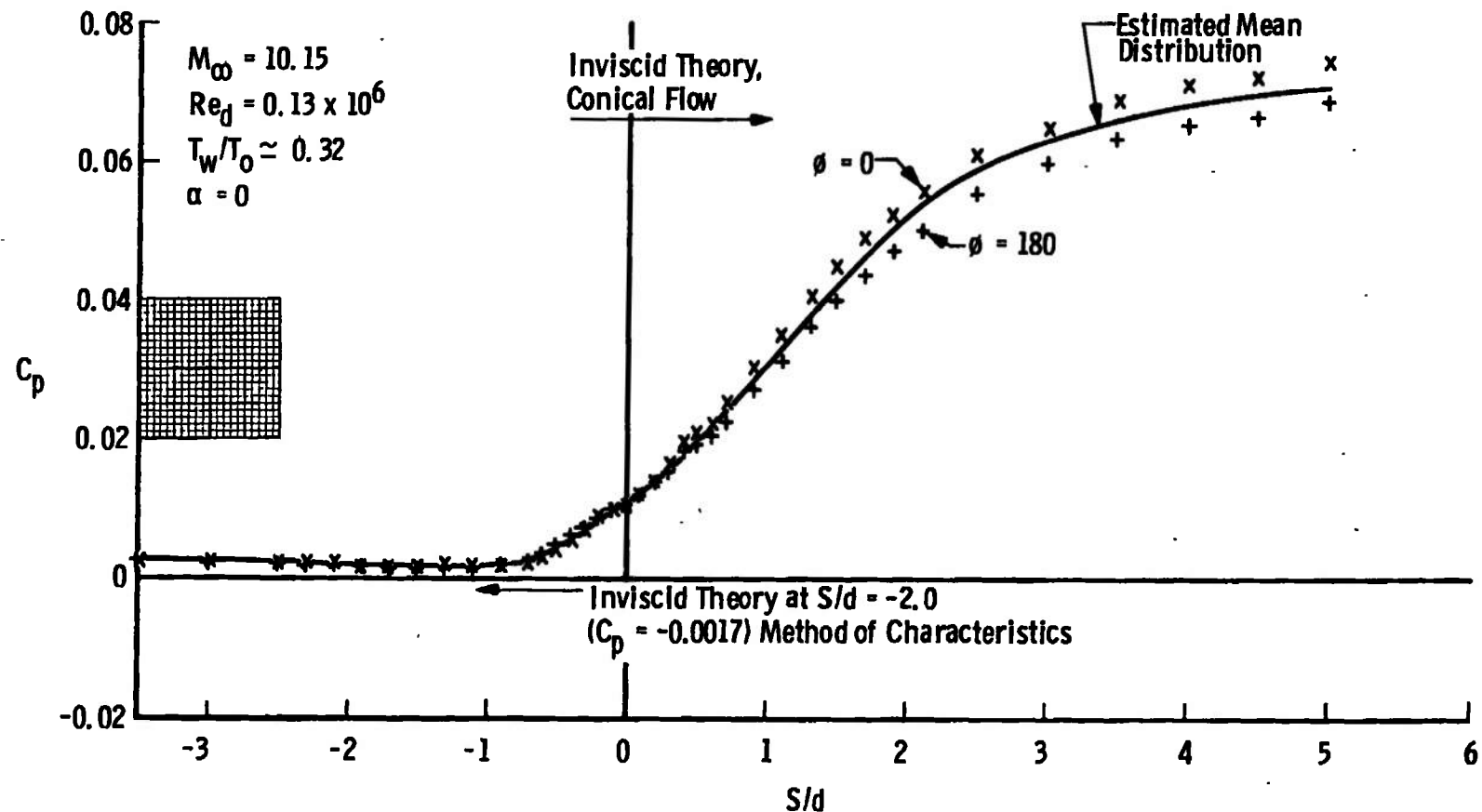
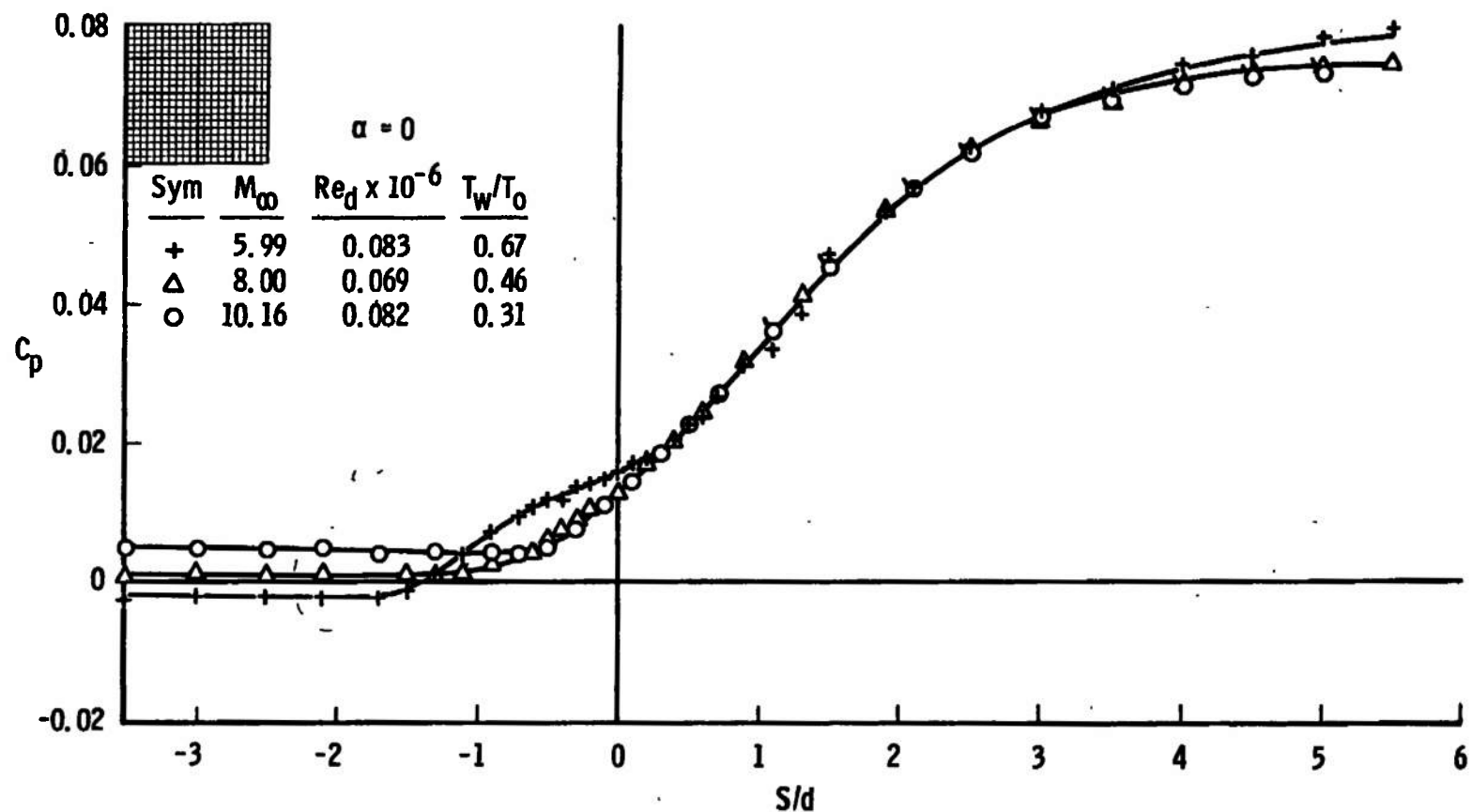
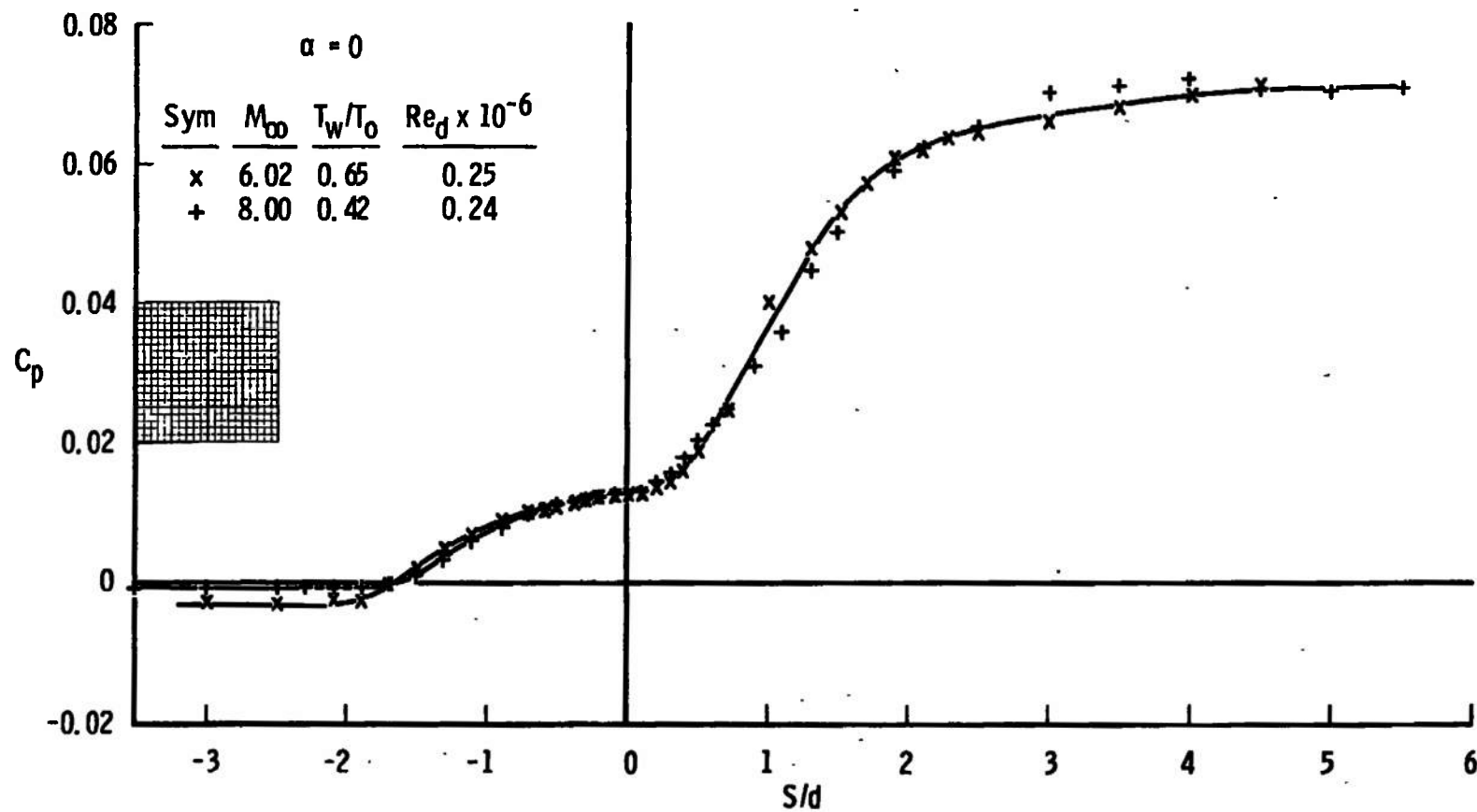


Fig. 7 Effect of Roll Angle on Surface Pressure Distribution for Near Ambient Wall Temperature at Mach 10



a. Low Reynolds Number, $0.069 \leq Re_d \times 10^{-6} \leq 0.083$

Fig. 8 Surface Pressure Distributions at Different Mach Numbers for Near Ambient Wall Temperatures



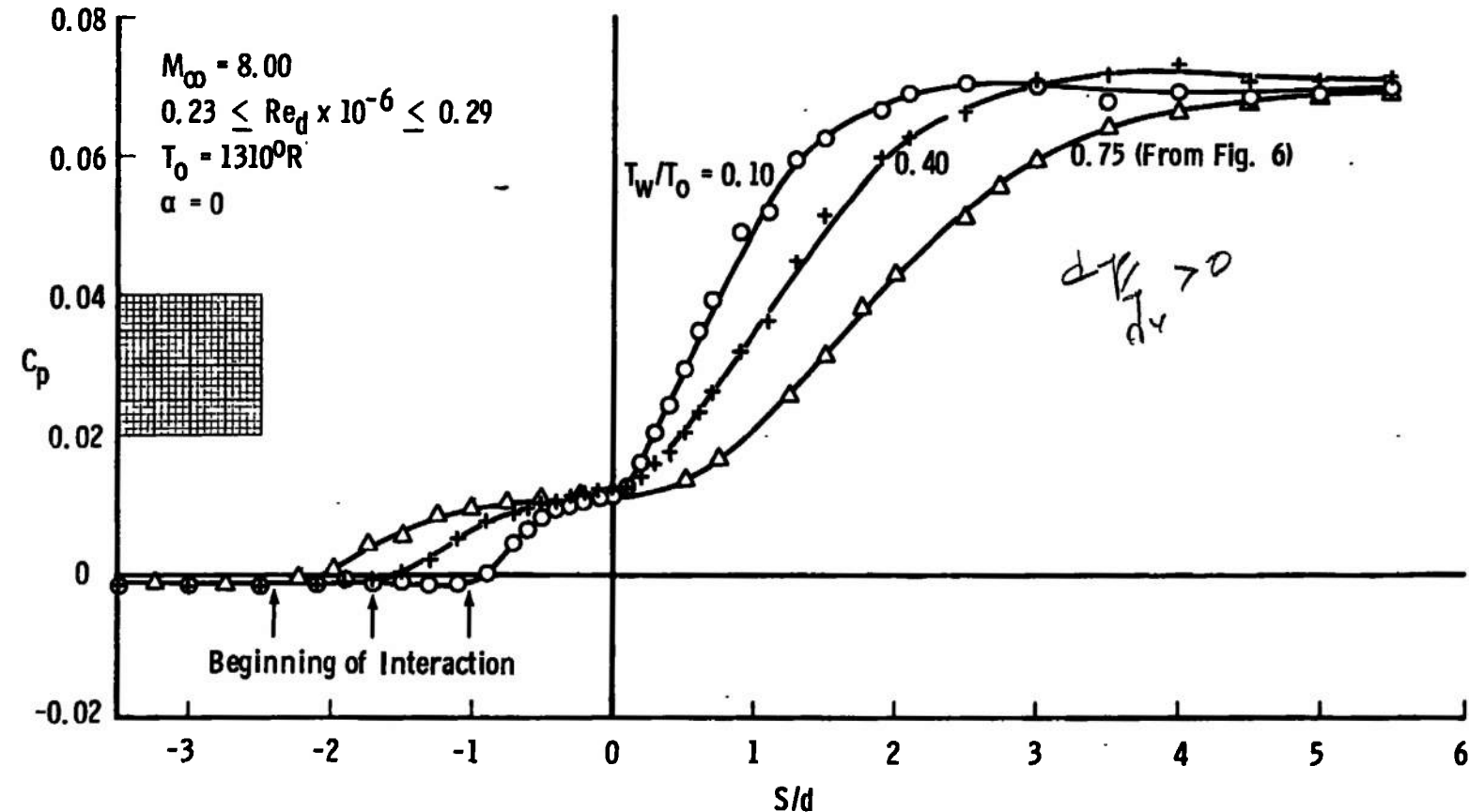
b. High Reynolds Number, $Re_d \approx 0.25 \times 10^6$

Fig. 8 Concluded

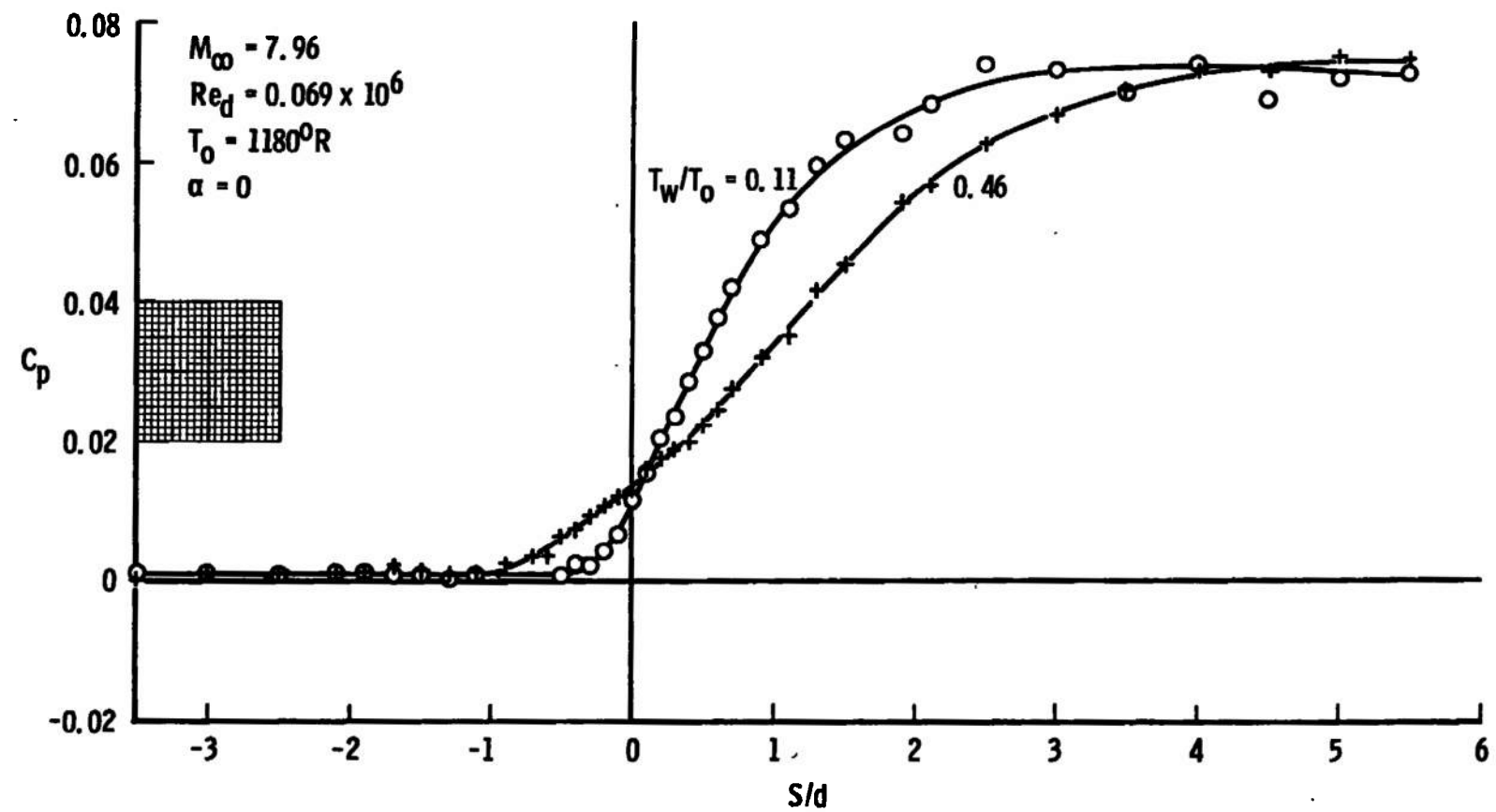
The influence of wall cooling on the overall interaction for constant Reynolds numbers and Mach numbers is clearly demonstrated by the pressure distributions given in Figs. 9a and b. There are two obvious effects generally evident. First, the pressure gradients were conspicuously increased; secondly, the region over which the interaction takes place was substantially reduced. The data in Fig. 9c are presented to show how transition can affect these trends. As already noted in the discussion of Fig. 4b, the flow in the region of reattachment at $Re_d = 0.38 \times 10^6$ was transitional for the nearly adiabatic wall temperature. Since the flare pressure gradient changed such a relatively small amount with surface cooling (Fig. 9c), this indicates that wall cooling had a secondary influence on transitional flow reattachment. That is, reattachment was influenced to a greater extent by the change in boundary-layer velocity profile shape than by the reduction in thickness caused by the cooling. This would also explain why the beginning of the interaction changed so little, for it is certainly the reattachment location that controls the separation location for wedge-type separations.

Additional data like those already presented have been examined to estimate the distance upstream of the flare at which the pressure distribution first showed the onset of the free-interaction process associated with the flare-induced separation/interaction. These results, which are summarized in Fig. 10, show conclusively that wall cooling reduced the upstream influence, $(S/d)_o$, at all Reynolds numbers and that the upstream influence decreased as Reynolds number was reduced, regardless of the wall temperature ratio. To illustrate the effect of free-stream Mach number on the upstream influence, data for Mach 6 (from Fig. 9d), $Re_d = 0.083 \times 10^6$, are included in Fig. 10b. These data indicate that a substantial decrease in $(S/d)_o$ resulted when the Mach number was increased from 6 to 8 at fixed free-stream Reynolds number. If, however, a Reynolds number based on the local external conditions were used as the basis of comparison, these Mach 6 data should be compared with Mach 8 data at a free-stream Reynolds number of about 0.14×10^6 because of the higher total pressure loss across the bow wave at Mach 8. On this basis, the data indicate an almost negligible effect of Mach number.

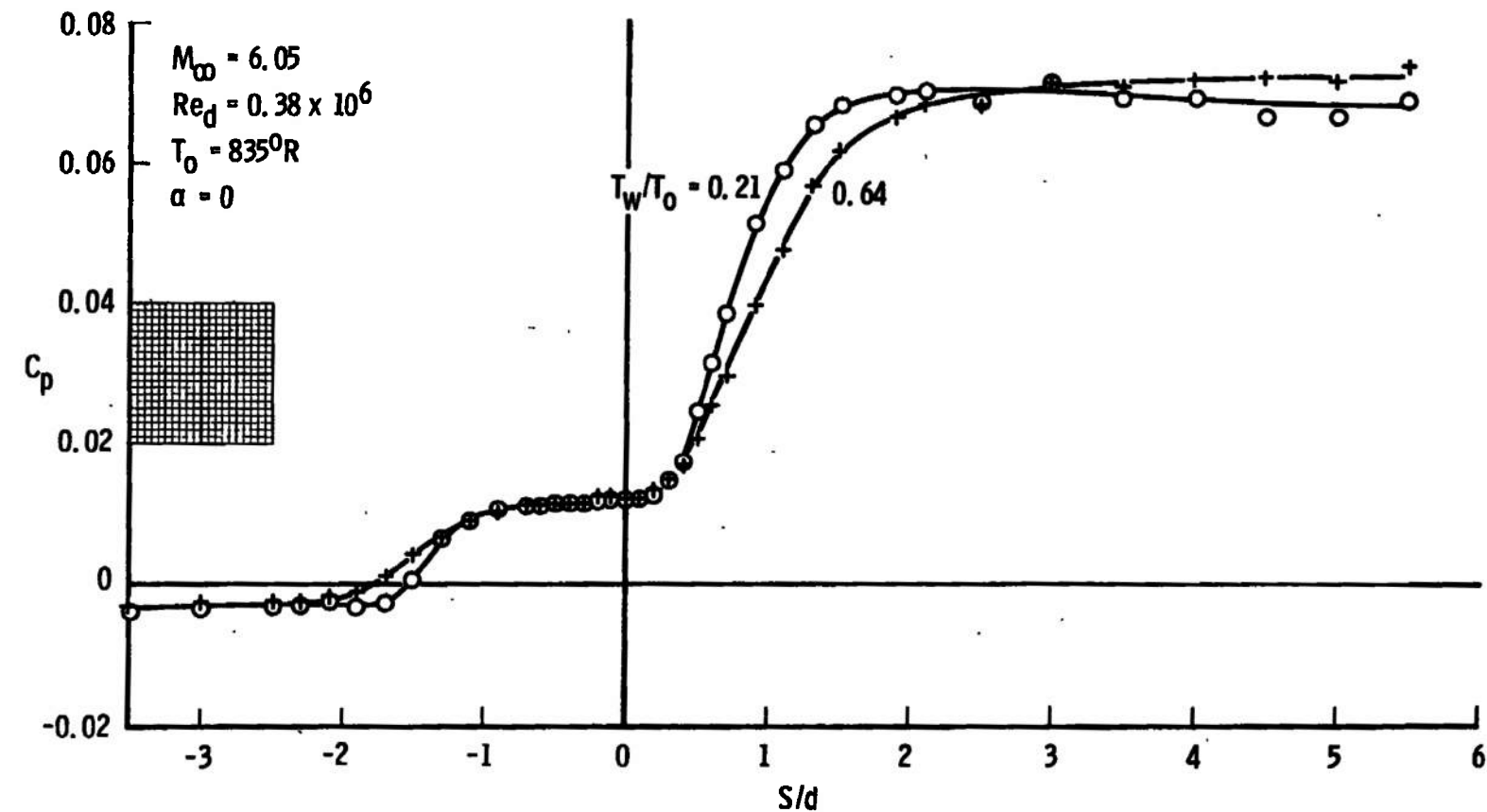
The shadowgraph pictures in Figs. 11 and 12 are presented to illustrate the effects of wall temperature and Mach number on the boundary layer. These pictures show that turbulence was easily identified at both Mach 8 (in the wake near the sting), Fig. 11a, and at Mach 6 (on the flare near its midpoint), Fig. 12a. The pictures in Fig. 12 at Mach 6 show that wall cooling produced a substantial delay in the onset of transition.



a. Mach 8, Maximum Reynolds Number
Fig. 9 Surface Pressure Distributions at the Wall Temperature Extremes

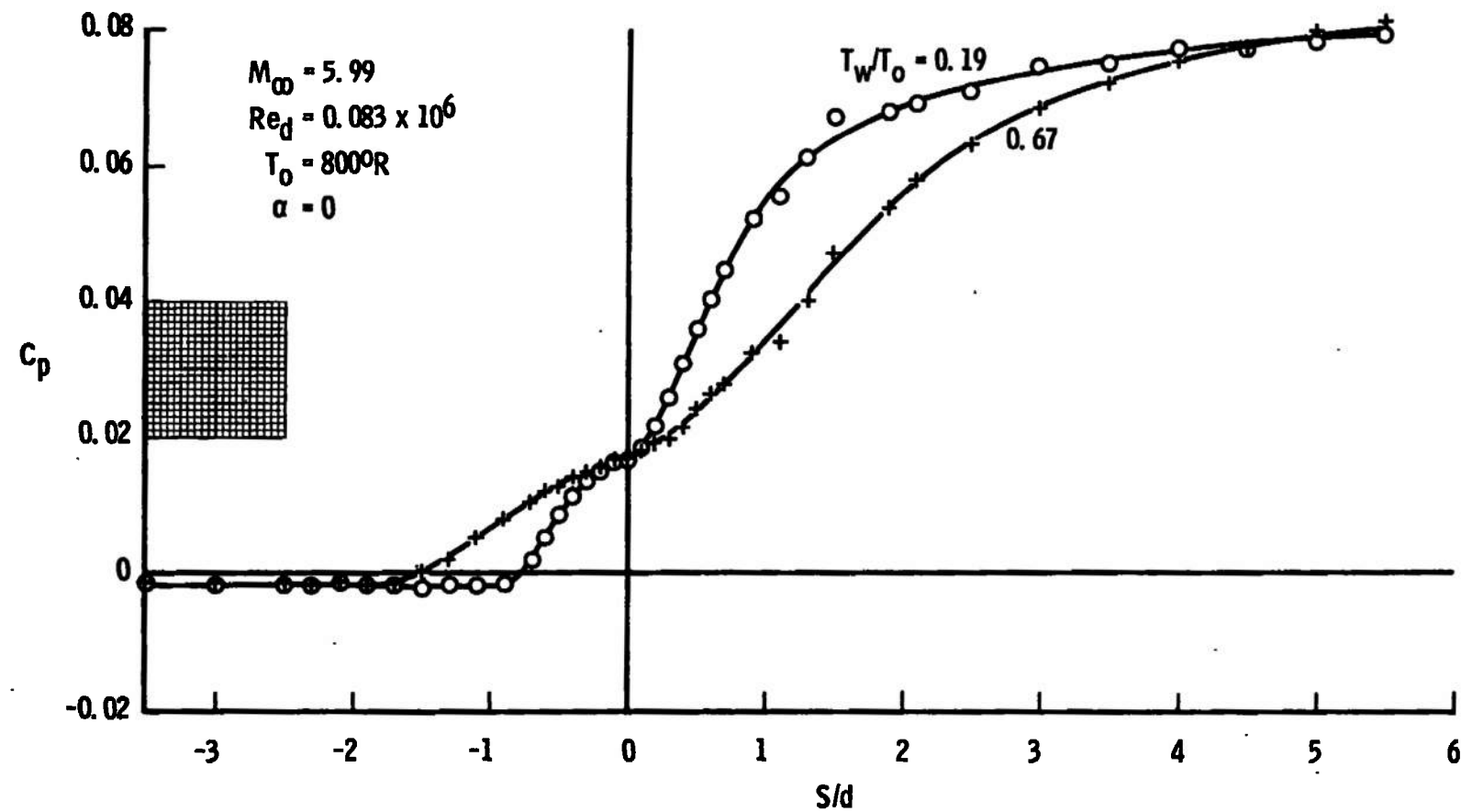


b. Mach 8, Minimum Reynolds Number
Fig. 9 Continued



c. Mach 6, Maximum Reynolds Number

Fig. 9 Continued



d. Mach 6, Minimum Reynolds Number

Fig. 9 Concluded

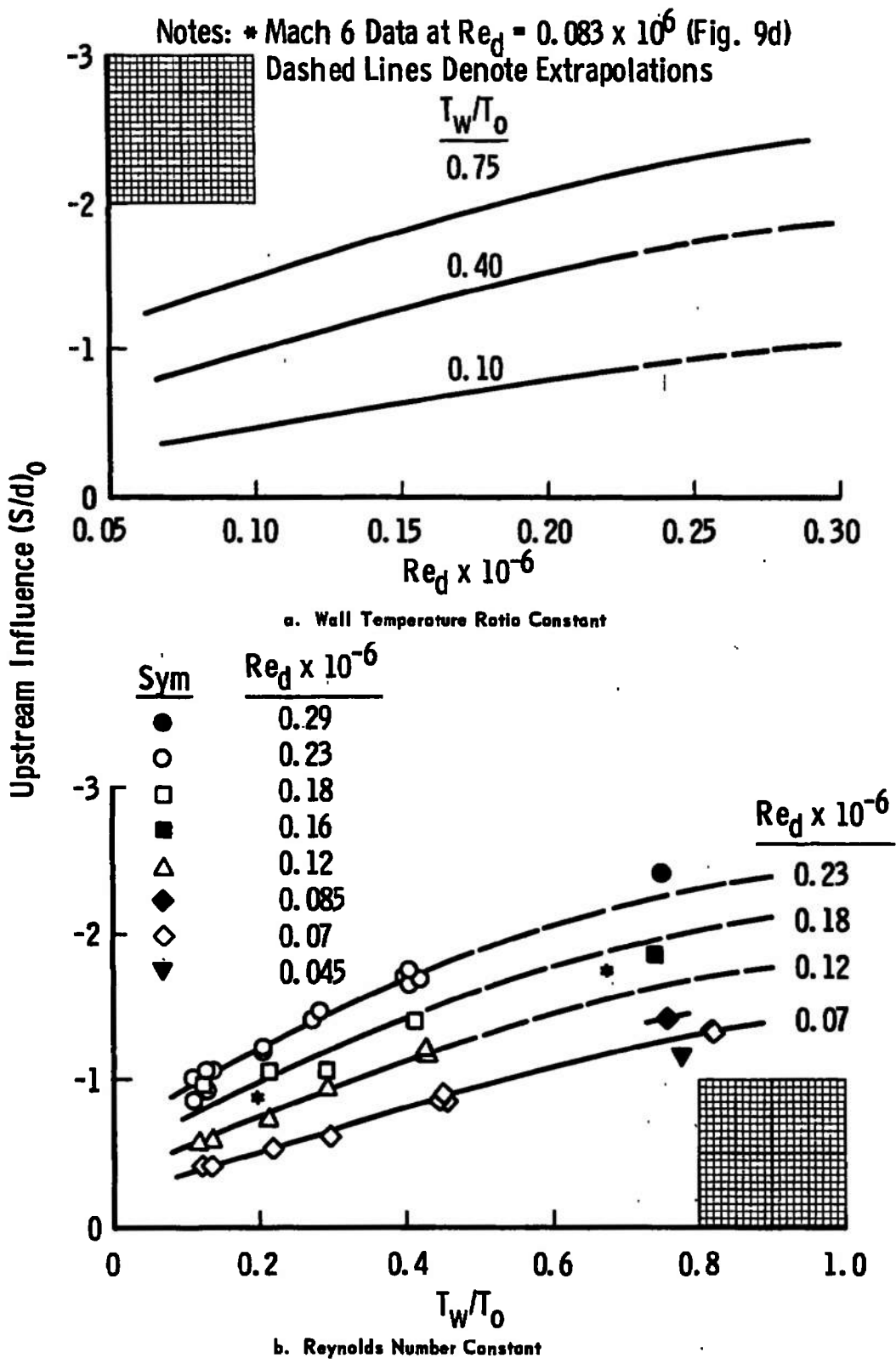
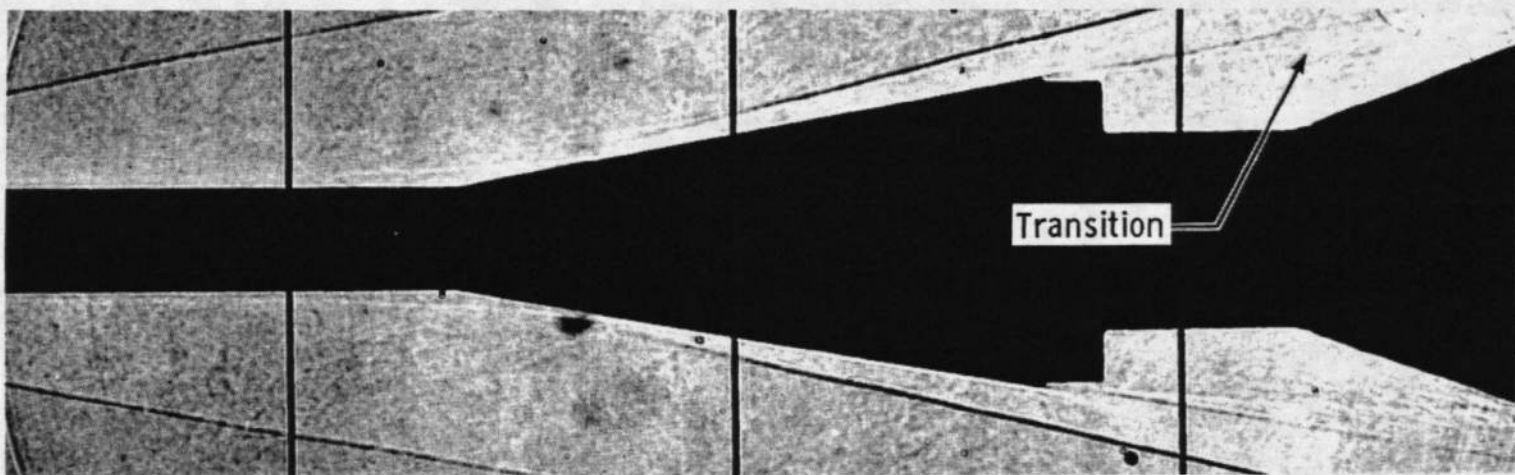
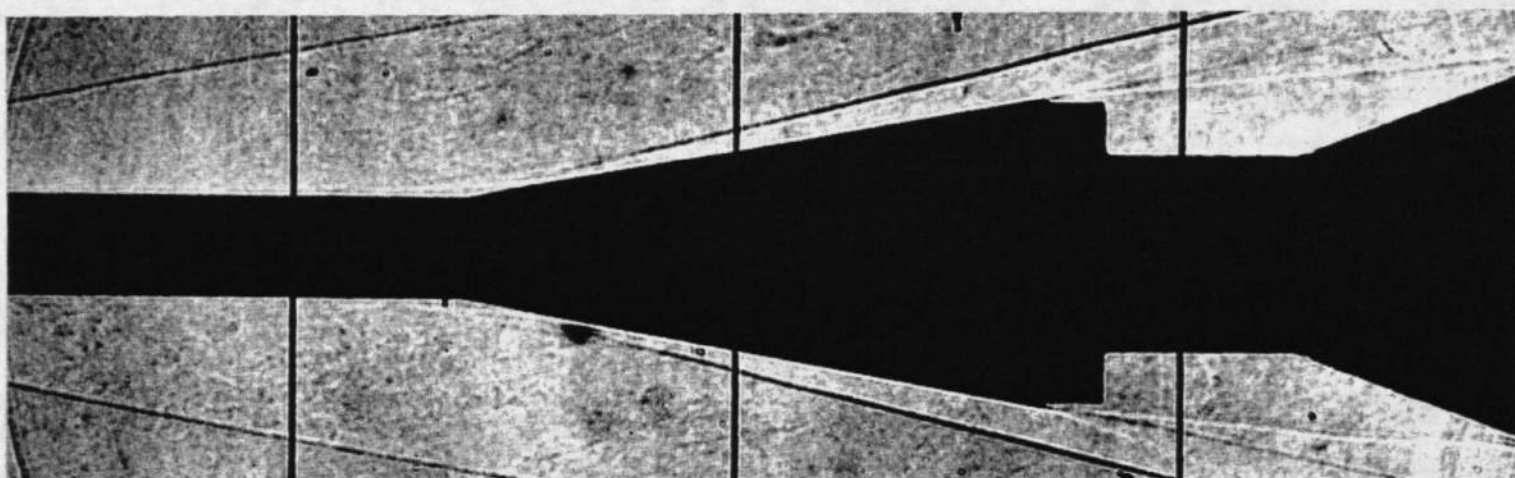


Fig. 10 Variation of the Upstream Influence with Reynolds Number and Heat Transfer at Mach 8 and Zero Incidence

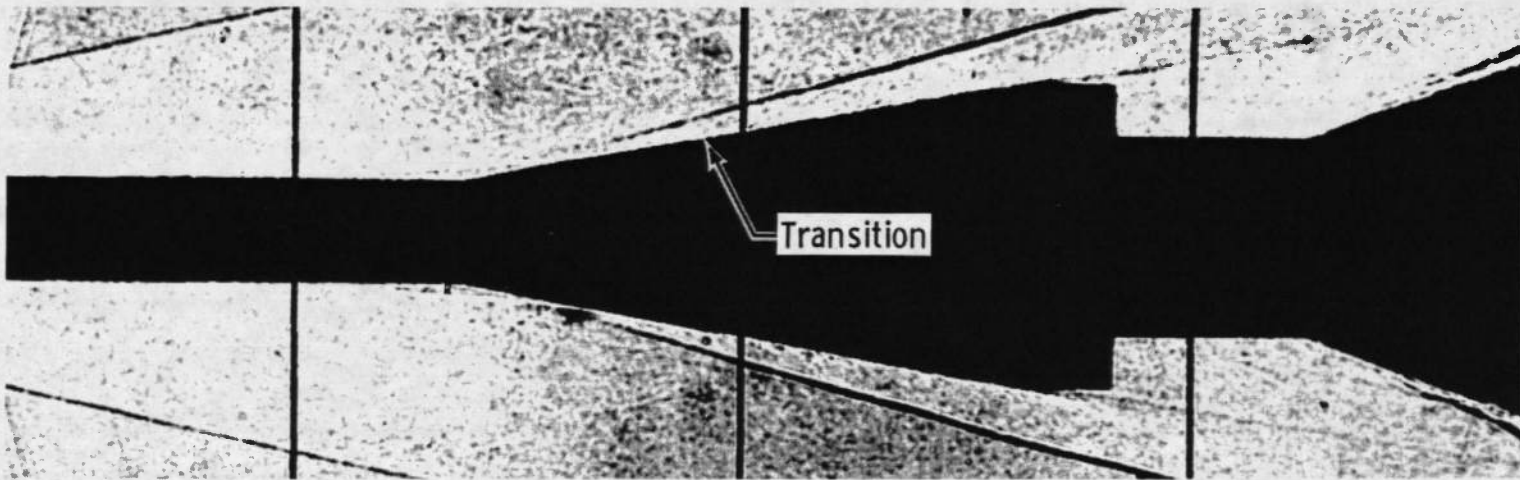


a. Near Ambient Wall Temperature ($T_w/T_o \sim 0.4$)

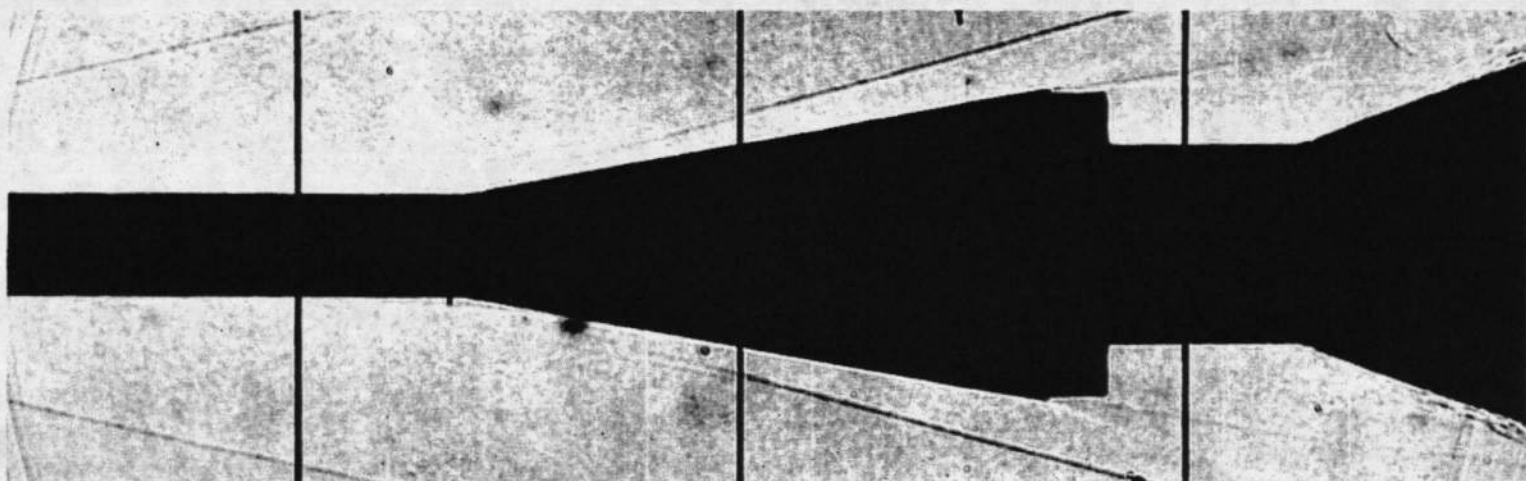


b. Minimum Wall Temperature ($T_w/T_o \sim 0.1$)

Fig. 11 Shadowgraph Pictures at Mach 8 for Different Wall Temperatures
at $Re_d = 0.23 \times 10^6$



a. Near Ambient Wall Temperature ($T_w/T_o \sim 0.7$)



b. Minimum Wall Temperature ($T_w/T_o \sim 0.3$)

Fig. 12 Shadowgraph Pictures at Mach 6 for Different Wall Temperatures
at $Re_d = 0.17 \times 10^6$

REFERENCES

1. Nielsen, J. N., Lynes, L. L., and Goodwin, F. K. "Calculation of Laminar Separation with Free Interaction by the Method of Integral Relations. Part II: Two-Dimensional Supersonic Non-adiabatic Flow and Axisymmetric Supersonic Adiabatic and Nonadiabatic Flows." AFFDL-TR-65-107, January 1966.
2. Gray, J. D. "Investigation of the Effect of Flare and Ramp Angle on the Upstream Influence of Laminar and Transitional Re-attaching Flows from Mach 3 to 7." AEDC-TR-66-190 (AD645840), January 1967.
3. Test Facilities Handbook (Sixth Edition). "von Kármán Gas Dynamics Facility, Vol. 4." Arnold Engineering Development Center, November 1966.
4. Lewis, J. E., Kubota, T., and Lees, L. "Experimental Investigation of Supersonic Laminar, Two-Dimensional Boundary-Layer Separation in a Compression Corner with and without Cooling." AIAA Journal, Vol. 6, No. 1, January 1968, pp. 7-14.

UNCLASSIFIED

Security Classification

DOCUMENT CONTROL DATA - R & D

(Security classification of title, body of abstract and indexing annotation must be entered when the overall report is classified)

| | | |
|---|--|---|
| 1. ORIGINATING ACTIVITY (Corporate author) Arnold Engineering Development Center ARO, Inc., Operating Contractor Arnold Air Force Station, Tennessee | | 2a. REPORT SECURITY CLASSIFICATION UNCLASSIFIED |
| | | 2b. GROUP N/A |
| 3. REPORT TITLE WALL COOLING EFFECTS ON AXISYMMETRIC LAMINAR REATTACHING FLOWS AT HYPERSONIC SPEEDS | | |
| 4. DESCRIPTIVE NOTES (Type of report and inclusive dates) December 1967 to April 22, 1968 - Final Report | | |
| 5. AUTHOR(S) (First name, middle initial, last name) J. Don Gray, ARO, Inc. | | |
| 6. REPORT DATE November 1968 | 7a. TOTAL NO. OF PAGES 31 | 7b. NO. OF REFS 4 |
| 8a. CONTRACT OR GRANT NO. F40650-69-C-0001 | 9a. ORIGINATOR'S REPORT NUMBER(S) AEDC-TR-68-135 | |
| b. PROJECT NO. 8219 | 9b. OTHER REPORT NO(S) (Any other numbers that may be assigned this report) N/A | |
| c. Program Element 6240533F | | |
| d. Task 821902 | | |
| 10. DISTRIBUTION STATEMENT This document has been approved for public release and sale; its distribution is unlimited. | | |
| 11. SUPPLEMENTARY NOTES Available in DDC | 12. SPONSORING MILITARY ACTIVITY AFFDL (FDCC) Wright-Patterson AFB, Ohio 45433 | |
| 13. ABSTRACT A flared (10-deg semiangle) axisymmetric body was tested at Mach 6, 8, and 10 in the von Kármán Gas Dynamics Facility to investigate the effect of model wall temperature on the existence of laminar flow separation and reattachment. The results consisted of longitudinal surface pressure distributions obtained at zero incidence. By varying the stagnation pressure, the influence of the free-stream Reynolds number on the extent of flow separation was also investigated. Extensive measurements were made at Mach 8 for Reynolds numbers (based on centerbody diameter) ranging from about 0.05 to 0.29 million and at wall temperatures from about 0.1 to 0.8 times the free-stream stagnation temperature. The results show that wall cooling increased substantially the pressure gradients at the separation and reattachment locations. The size of the interaction region (upstream influence) was found to decrease systematically with decreasing wall temperature ratio (Reynolds number constant) and to increase with increasing Reynolds number (constant wall temperature ratio). The effect of free-stream Mach number on the upstream influence (at fixed local Reynolds number and wall temperature) was indicated to be negligible. | | |

UNCLASSIFIED

Security Classification

| 14. KEY WORDS | LINK A | | LINK B | | LINK C | |
|--|--------|----|------------------------|----|--------|----|
| | ROLE | WT | ROLE | WT | ROLE | WT |
| 1. bodies of revolution -- flared afterbodies axisymmetric flow <u>pressure distribution</u> temperature wind tunnel tests hypersonic flow cooling Reynolds number | | | | | | |
| 2. Bodies of revolution -- Boundary layer transition | | | | | | |
| 3 " " | | | - Hypersonic flow, | | | |
| 4 " " | | | - Wall cooling | | | |
| 5 Boundary layer | | | - Transition | | | |
| 6 " " | | | - Reattachment | | | |
| 7 " " | | | - Wall Cooling effects | | | |
| 8 Walls -- Cooling effects | | | | | | |
| | 1 - | 2 | | | | |